Cancer Cell
Article

Genome-wide Loss-of-Function Screen Reveals an Important Role for the Proteasome in HDAC Inhibitor-Induced Apoptosis

Susan Fotheringham,[1] Mirjam T. Epping,[2] Lindsay Stimson,[1] Omar Khan,[1] Victoria Wood,[1] Francesco Pezzella,[3] René Bernards,[2] and Nicholas B. La Thangue[1,*]
[1]Laboratory of Cancer Biology, Department of Clinical Pharmacology, Medical Sciences Division, University of Oxford, Old Road Campus Research Building, Oxford OX3 7DQ, UK
[2]Division of Molecular Carcinogenesis, The Netherlands Cancer Institute, Plesmanlaan 121, Amsterdam, CX 1066, The Netherlands
[3]Cancer Research UK Tumour Pathology Unit, John Radcliffe Hospital, Oxford OX3 9DU, UK
*Correspondence: nick.lathangue@ndcls.ox.ac.uk
DOI 10.1016/j.ccr.2008.12.001

SUMMARY

Aberrant acetylation has been strongly linked to tumorigenesis, and the modulation of acetylation through targeting histone deacetylases (HDACs) is gathering increasing pace as a viable therapeutic strategy. A genome-wide loss-of-function screen identified HR23B, which shuttles ubiquitinated cargo proteins to the proteasome, as a sensitivity determinant for HDAC inhibitor-induced apoptosis. HR23B also governs tumor cell sensitivity to drugs that act directly on the proteasome. The level of HR23B influences the response of tumor cells to HDAC inhibitors, and HR23B is found at high levels in cutaneous T cell lymphoma in situ, a malignancy that responds favorably to HDAC inhibitor-based therapy. These results suggest that deregulated proteasome activity contributes to the anticancer activity of HDAC inhibitors.

INTRODUCTION

The recognition that aberrant epigenetic control is an important determinant in attaining the malignant phenotype has stimulated intense efforts to develop mechanism-based drugs that regulate epigenetic pathways in cancer (Inche and La Thangue, 2006). Reversible histone acetylation represents a key underpinning mechanism involved in epigenetic control. One of the most rapidly progressing areas, from the perspective of anticancer agents, has been seen in the development of small-molecule inhibitors of histone deacetylase (HDAC) enzymes (Marks and Jiang, 2005; Bolden et al., 2006). In cell-based assays, HDAC inhibitors have a striking effect on tumor cell proliferation, frequently promoting apoptosis (Richon, 2006; Marks and Breslow, 2007). Consequently, HDAC inhibitors have entered clinical studies. While the clinical picture is quite variable and the outcome of HDAC inhibitor-based therapy complex, it is significant that, at the current time, certain types of tumors are known to undergo a favorable response. Hematological malignancies appear to be particularly sensitive, and in this respect vorinostat (suberoylanilide hydroxamic acid, or SAHA) has already shown promising clinical effects in late-stage cutaneous T cell lymphoma (CTCL; Mann et al., 2007; Khan and La Thangue, 2008).

However, significant gaps remain in our understanding of how HDAC inhibitors exert antitumor activity, and the key mechanisms and pathways through which HDAC inhibition blocks tumor cell proliferation have not been well defined. Although deregulating chromatin is likely to be involved in tumor cell killing, a variety of other mechanisms and pathways that contribute to the cellular effects of HDAC inhibitors have been described (Richon, 2006; Inche and La Thangue, 2006; Minucci and Pelicci, 2006; Bolden et al., 2006; Xu et al., 2007). Moreover, elucidating the critical pathways that govern tumor cell killing should assist in

SIGNIFICANCE

It is becoming increasingly clear that acetylation, and specifically histone deacetylation, regulates many key pathways that drive tumorigenesis. Histone deacetylase (HDAC) inhibitors cause tumor cells to enter apoptosis, and there is great interest in HDAC inhibitor-based therapies as a new type of anticancer agent. However, many details of the pathways through which HDAC inhibition causes tumor cell death remain to be resolved. Consequently, understanding of the clinical utility of HDAC inhibitors has been hampered, and there is a pressing need to identify mechanism-related biomarkers. Our study has elucidated an unexpected yet central role for the proteasome and the proteasome-targeting protein HR23B in HDAC inhibitor-induced apoptosis. HR23B might provide a useful biomarker for identifying tumors that exhibit a favorable response to HDAC inhibitors.

clarifying the clinical spectrum of responsive tumors, which for the most part remains unclear.

It was against this background that we performed a genome-wide loss-of-function screen to identify genes that govern the sensitivity of tumor cells to HDAC inhibitors. We reasoned that genes identified through the screen might provide insights into the cellular pathways and molecular mechanisms affected by HDAC inhibition. Our results revealed a functionally important pathway involving the proteasome, specifically the proteasome-targeting activity of HR23B, and its potential role in HDAC inhibitor-induced cell death. The level of HR23B influences the outcome of HDAC inhibitor treatment, and proteasome activity is deregulated through a pathway that involves HR23B in HDAC inhibitor-treated cells. Our study suggests that aberrant proteasome activity contributes to the anticancer activity of HDAC inhibitors and provides a rational basis for identifying patients that gain clinical benefit from HDAC inhibitor-based therapies.

RESULTS

Loss-of-Function Screen for HDAC Inhibitor Sensitivity Genes

The loss-of-function screen used a shRNA library targeting the vast number of human genes involved in cancer, in which each shRNA induces strong and specific suppression of gene expression over prolonged periods of time (Berns et al., 2004). We configured the screen to allow the identification of genes that influence the sensitivity of U2OS cells to HDAC inhibitors. This rationale was based on the fact that silencing genes required for HDAC inhibitor-induced apoptosis would allow cells to survive in the presence of the drug (Figure 1A). Surviving cells could then be isolated, and the relevant genes could be identified and thereafter validated in functional assays as determinants of HDAC inhibitor sensitivity; the output of the screen is described in Figure S1 available online.

We focused our attention on a shRNA vector targeting HR23B, which conferred resistance to HDAC inhibitor-induced apoptosis in U2OS cells. To determine whether expression of the gene targeted by the shRNA sequence was in fact reduced, the level of the HR23B protein was investigated. The HR23B protein level was low in cells stably expressing HR23B-specific shRNA (Figure 1B). The effect of the shRNA sequence derived from stable expression was compared to that of a siRNA targeting the same sequence (SP) and to another siRNA (2) derived from a different region of the HR23B RNA; both siRNAs depleted HR23B (Figure 1C). Lamin siRNA (L) served as an unrelated gene-specific control siRNA.

In order to validate the role of HR23B in regulating sensitivity to HDAC inhibition, we assessed the effect of HR23B depletion using both HR23B siRNAs on HDAC inhibitor-induced apoptosis. The introduction of either siRNA against HR23B RNA, including the SP siRNA, reduced the sensitivity of U2OS cells to undergo apoptosis in response to HDAC inhibitor treatment (Figure 1D). Furthermore, mouse embryonic fibroblasts (MEFs) derived from *HR23B*$^{-/-}$ knockout mice (Ng et al., 2002) were less sensitive to HDAC inhibitor-induced apoptosis than their wild-type (WT) counterparts (Figure 1E). HR23B is one of two human homologs of *Saccharomyces cerevisiae* Rad23 (Schauber et al., 1998; Sugasawa et al., 1997). However, HR23A siRNA did not affect HDAC inhibitor-induced apoptosis (Figures 1F and 1G), indicating that HR23A and HR23B take on distinct roles during HDAC inhibitor-induced apoptosis in this cell system.

Having established that HR23B is functionally important in regulating sensitivity to HDAC inhibitors, we next assessed the effect of HDAC inhibition on HR23B. There was an increase in the level of HR23B in U2OS cells treated with the HDAC inhibitor SAHA (Figure 2A), which reflected higher levels of HR23B immunostaining (Figure 2B). The increased level of HR23B was seen in a variety of other cell types treated with HDAC inhibitors, including A2780 (ovarian), MCF7 (breast), and H460 (lung) tumor cells (Figure S2A). Other HDAC inhibitors, including PXD101 and valproic acid (VPA) (Carey and La Thangue, 2006), together with the natural product trichostatin A (TSA), had a similar effect on HR23B without any apparent effect on RNA levels (Figures 2C and 2D). Moreover, HR23B is acetylated, and acetylation occurred in both untreated and treated cells at 48 hr (Figures 2E and 2F), with a modest increase in acetylation occurring at 24 hr treatment (Figure S2B). Thus, HR23B is targeted by the acetylation machinery, and HR23B is regulated through a posttranscriptional mechanism in HDAC inhibitor-treated cells.

It was, however, important to assess the regulation of HR23B by other types of agents that kill cancer cells, particularly those that also induce apoptosis, to exclude the possibility that HR23B is generally affected by drug-induced apoptosis. In cells treated under apoptosis-inducing conditions (Figure S2C) with different anticancer agents, including etoposide, bleomycin, doxorubicin, and ultraviolet (UV) light, there was little effect on HR23B levels (Figures 2G and 2H).

Role of HR23B in HDAC Inhibitor-Treated Cells

HR23B participates in nucleotide excision repair (NER; Sugasawa et al., 1997). It binds to the xeroderma pigmentosum complementation group C (XPC) protein, which then interacts with damaged DNA (Sugasawa et al., 1997), and has another important function related to a role in targeting ubiquitylated substrates to the proteasome (Schauber et al., 1998; Chen and Madura, 2002; Hiyama et al., 1999). A ubiquitin-like domain in the N-terminal region of HR23B interacts with the proteasome, and two ubiquitin-associated domains located in an internal and C-terminal region (Chen et al., 2001; Wilkinson et al., 2001; Chen and Madura, 2002) allow HR23B to shuttle proteins destined for degradation to the proteasome. To gain insight into the property of HR23B that is relevant for HDAC inhibitor sensitivity, the effect of HDAC inhibition on XP4PA cells was investigated. XP4PA cells carry a defective *XPC* gene and exhibit low NER activity, and as a consequence, the importance of HR23B in NER is reduced in these cells (Li et al., 1993). However, XP4PA cells were as sensitive to HDAC inhibitor-induced apoptosis as control human M2C5 fibroblasts and U2OS cells, which have normal XPC and NER activity (Figures 3A and 3Ba), and HR23B was similarly induced in XP4PA cells upon treatment with HDAC inhibitors (Figure 3Bc) when compared to both U2OS and M2C5 cells (Figures 3Bb and 3Bd). These results suggest that HDAC inhibitors do not induce apoptosis through an HR23B-dependent pathway that relies on NER activity.

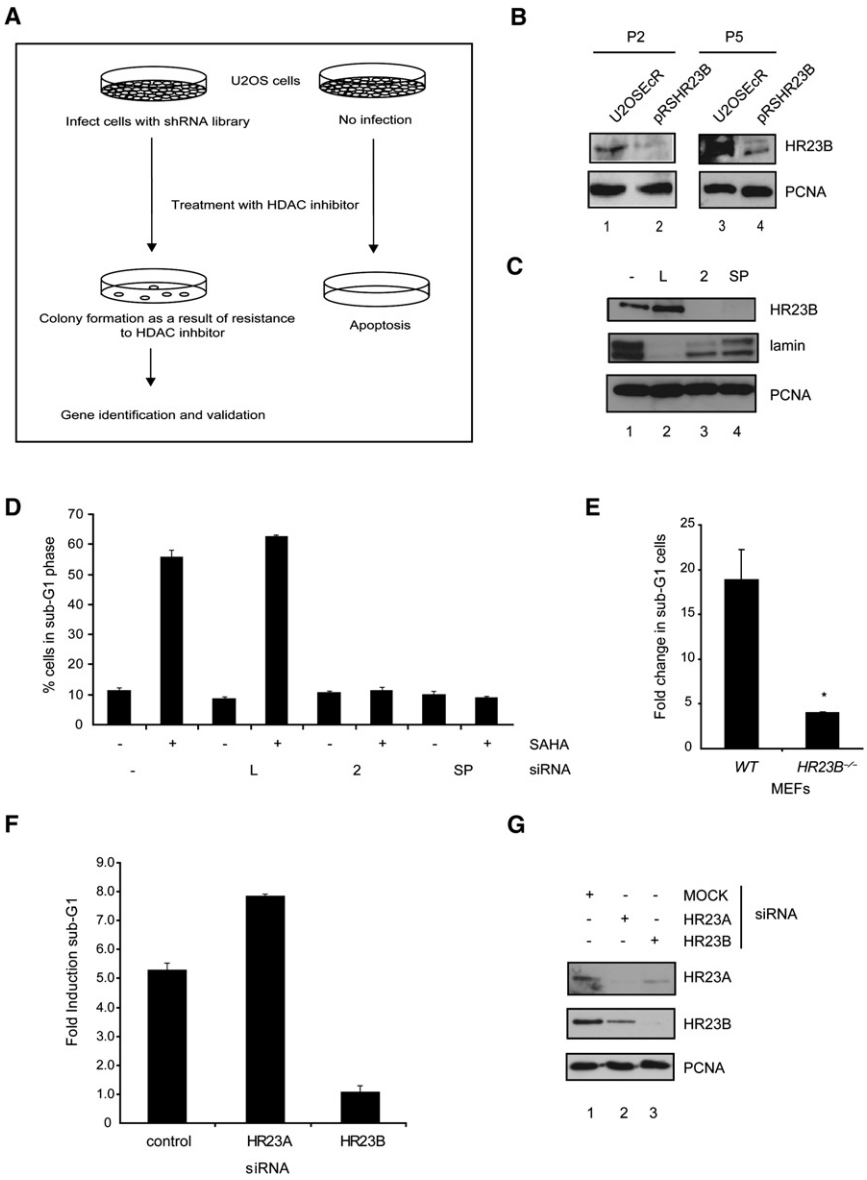

Figure 1. HDAC Inhibitor shRNA Loss-of-Function Screen

(A) U2OSEcR cells were infected with the pRetroSuper shRNA library and then treated with 2 μM suberoylanilide hydroxamic acid (SAHA) for up to 25 days, conditions in which apoptosis occurred. Colonies were harvested, and the genes targeted by the shRNA were identified. (Further details of the output from the shRNA screen can be found in Figure S1.)

(B) Validation of HR23B knockdown. The immunoblots show the level of HR23B in pRetroSuper HR23B U2OS cells (pRSHR23B) derived from the shRNA screen after two (P2) or five (P5) passages. PCNA was used as a loading control, and the level of HR23B is shown for comparison in the parental line (U2OSEcR).

(C) Transient knockdown of HR23B with siRNA. siRNAs against different regions in HR23B, including a siRNA (referred to as SP) representing the sequence in the original pRetroSuper HR23B vector isolated in the screen in (A) and siRNA 2 against an unrelated sequence in HR23B RNA, were compared for level of HR23B knockdown at 48 hr after treatment in U2OS cells. Lamin (L) was used as a siRNA control and PCNA as a loading control; – indicates untreated cells.

(D) Levels of sub-G1 apoptotic cells determined by fluorescence-activated cell sorting (FACS) after treating U2OS cells with either lamin (L) or HR23B siRNA (2 and SP; as described in [C]) for 48 hr followed by treatment with SAHA (5 μM) for 48 hr. n = 3; error bars = SEM.

(E) Levels of sub-G1 apoptotic cells determined by FACS after treating either wild-type (WT) or *HR23B*$^{-/-}$ mouse embryonic fibroblasts (MEFs) with SAHA (30 μM) for 48 hr, compared to untreated cells. The absolute level of sub-G1 cells was 52% in WT MEFs and 7% in *HR23B*$^{-/-}$ MEFs. n = 4; error bars = SEM. *$p < 0.05$ by unpaired Student's t test.

(F) Fold induction of sub-G1 phase of the cell cycle as measured by FACS analysis after treatment of U2OS cells with control (–), HR23A, or HR23B siRNA as indicated for 48 hr, followed by treatment with 5 μM SAHA for a further 48 hr. The absolute level of sub-G1 cells for control, HR23A, and HR23B siRNA treatment was 52%, 70%, and 15%, respectively. n = 4; error bars = SEM.

(G) Immunoblot showing protein levels of HR23A, HR23B, and PCNA for the experiment described in (F).

Proteasome Activity in HDAC Inhibitor-Treated Cells

To test whether HDAC inhibitors influence the interaction between HR23B and the proteasome, we investigated the association between HR23B and the proteasome, with which HR23B interacts via the ubiquitin-like domain, allowing HR23B to target cargo proteins to the proteasome (Wilkinson et al., 2001; Chen and Madura, 2002). There was an increase in the level of HR23B bound to the proteasome in HDAC inhibitor-treated cells when the immunoprecipitating antibody was anti-HR23B (~4-fold; Figure 3Ca), and HR23B levels were similarly increased when the immunoprecipitating antibody recognized the 20S core α6 subunit (~4-fold; Figure 3Cb). The interaction between HR23B and the S5a 19S proteasome subunit (Fujiwara et al., 2004) was also observed to increase after HDAC inhibitor treatment (Figure S1D). The association of HR23B with the proteasome therefore increases in HDAC inhibitor-treated cells.

To test the idea that proteasome activity is aberrant in HDAC inhibitor-treated cells, we used an HEK293 cell line expressing an unstable GFP, GFP^{u}, in which GFP is fused to the Ch1 degron sequence (Gilon et al., 1998; Bence et al., 2001). The Ch1 sequence destabilizes GFP by targeting it for degradation via the ubiquitin-proteasome pathway; thus, the level of GFP provides an independent measure of proteasome activity (Bence et al., 2001). As expected, GFP^{u} was stabilized in the presence of the

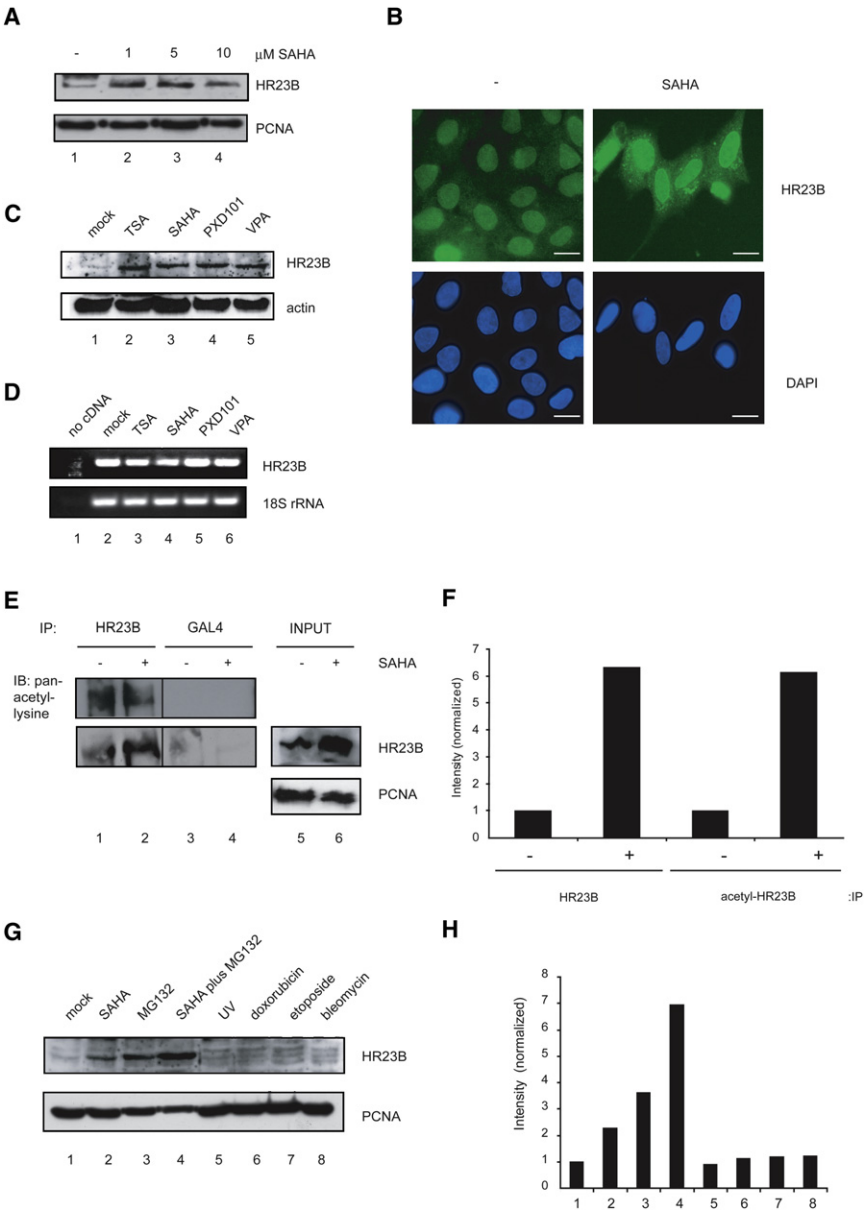

Figure 2. HR23B Regulates Sensitivity to HDAC Inhibitors

(A) HR23B protein levels in SAHA-treated cells. Immunoblots show HR23B in U2OS cells after treatment with 0 (−), 1, 5, or 10 μM SAHA for 48 hr (fold change in HR23B levels relative to 0 was 6, 5.5, and 4, respectively). PCNA was used as a loading control. The example shown is representative of three different experiments.

(B) HR23B protein levels and localization in SAHA-treated cells. Immunostaining shows the level of HR23B in U2OS cells before and after treatment with 5 μM SAHA for 48 hr. Nuclei were located by comparison to DAPI staining. Scale bars = 10 μm.

(C) HR23B protein levels in U2OS cells treated with different HDAC inhibitors. Immunoblots show increased protein levels of HR23B after treatment for 48 hr with trichostatin A (TSA) (1 μM), SAHA (5 μM), PXD101 (1 μM), and valproic acid (VPA) (10 mM), with actin as a loading control (fold change in HR23B levels relative to mock was 7, 5.2, 6.5, and 6.5, respectively).

(D) HR23B is not regulated at the RNA level upon HDAC inhibition. RT-PCR shows levels of HR23B RNA after treatment of U2OS cells for 48 hr with TSA, SAHA, PXD101, or VPA at the concentrations described in (C) for 48 hr, with 18S rRNA as a loading control (fold change in HR23B RNA relative to 18S rRNA was 0.98, 0.99, 1.2, and 1.4, respectively).

(E) HR23B is acetylated. Immunoprecipitation from U2OS cell extracts with anti-HR23B or GAL4 antibody (as a nonspecific control) from cells either untreated or treated with 5 μM SAHA for 48 hr is shown. Immunoblotting was subsequently performed with an antibody against pan-acetyl-lysine. Input levels of HR23B and PCNA as a loading control are also shown.

(F) Quantification of relative levels presented in (E). The level of acetylated or total HR23B in the immunoprecipitate from untreated cells (−; lane 1 in [E]) was given an arbitrary value of 1 and used to calculate the fold increase in SAHA-treated cells (+).

(G) HR23B protein levels are not regulated by DNA-damaging agents. Immunoblots show HR23B protein levels after treatment of U2OS cells for 48 hr with SAHA (5 μM), MG132 (0.5 μM), combination of SAHA (5 μM) and MG132 (0.5 μM), ultraviolet (UV) light (50 J), doxorubicin (10 μM), etoposide (20 μM), or bleomycin (1 μg/ml). PCNA was used as a loading control.

(H) Quantification of relative protein levels in (G) with respect to PCNA.

proteasome inhibitor bortezomib (Figure 3D), confirming that the level of GFP^u reflects the ability of the proteasome to degrade proteins. Upon titration of different HDAC inhibitors (TSA, SAHA, and PXD101), there was a significant increase in the level of GFP^u protein relative to control treatment (Figure 3E); moreover, the increase in GFP^u levels did not result from altered RNA levels (Figure 3F).

We next assessed the effect of HDAC inhibitors on proteasome activity in vitro. Purified proteasomes from untreated cells were not directly affected by HDAC inhibitors, in contrast to the effect of bortezomib, which blocked proteasome activity (Figure 3Ga). However, proteasomes purified from HDAC inhibitor-treated cells displayed decreased proteolytic activity (Figure 3Gb), which is compatible with the results derived from the GFP^u HEK293 cell line (Figure 3E), namely that proteasome activity is compromised in HDAC inhibitor-treated cells.

To investigate the role of HR23B in the HDAC inhibitor-dependent effects on proteasome activity, we introduced HR23B siRNA into the GFP-u1 HEK293 cell line and monitored the effects on GFP^u levels. The increased levels of GFP^u observed in HDAC inhibitor-treated cells were reduced upon the depletion of HR23B (Figure 3H). These results suggest therefore that

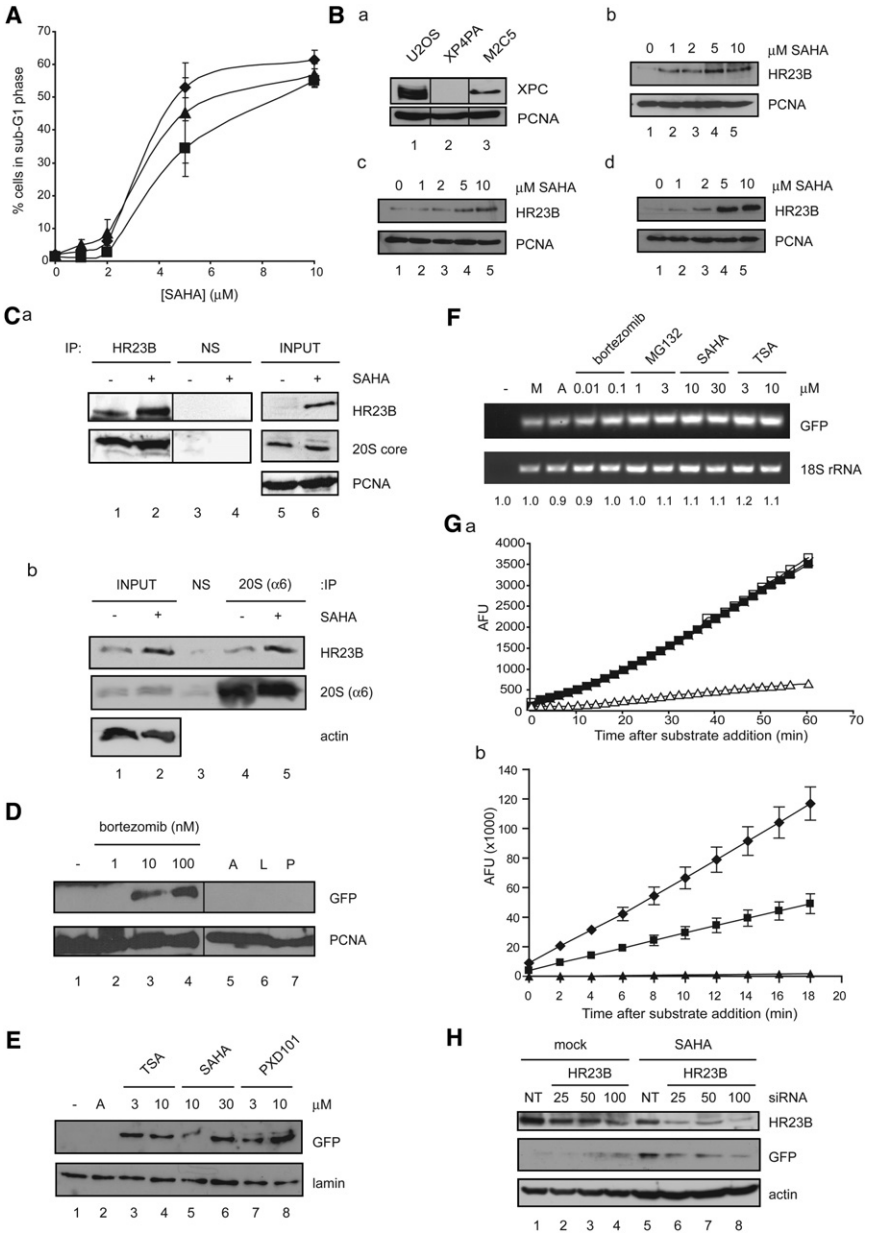

Figure 3. Proteasome Activity in HDAC Inhibitor-Treated Cells

(A) Loss of XPC does not affect cell sensitivity to SAHA. Graph shows the percentage of XP4PA (▲), M2C5 (■), and U2OS (◆) cells in sub-G1 as determined by FACS after treatment with increasing concentrations of SAHA (0, 1, 2, 5, and 10 μM) for 48 hr. The values obtained in the different cell lines were not significantly different at each concentration of SAHA. n = 4; error bars = SEM.

(Ba–Bd) Loss of XPC does not impact the regulation of HR23B levels after SAHA treatment. Immunoblots show expression levels of XPC in the indicated cell types (Ba) and levels of HR23B after treatment with increasing concentrations of SAHA for 48 hr in U2OS (Bb), XP4PA (Bc), and M2C5 (Bd) cells, with PCNA as a loading control.

(Ca and Cb) HDAC inhibitor treatment and binding of HR23B to the 20S proteasome.

(Ca) Immunoprecipitation of U2OS cells with anti-HR23B or control anti-GAL4 antibody (NS) either untreated (–) or treated (+) with SAHA (5 μM) for 48 hr and subsequently immunoblotted with anti-HR23B or 20S proteasome antibody. Input levels are shown together with PCNA as a loading control (lanes 5 and 6). There was a 4-fold increase in the level of HR23B associated with the 20S proteasome in SAHA-treated cells.

(Cb) U2OS cells were treated as described above, and extracts were immunoprecipitated with anti-20S core α6 subunit or control antibody and subsequently immunoblotted with anti-HR23B or anti-20S core α6 subunit antibody. Input levels are shown together with actin as a loading control (lanes 1 and 2). There was a 4-fold increase in the level of HR23B associated with the 20S proteasome.

(D) GFP-u1 HEK293 cells express an unstable GFP, GFP^u, after treatment with bortezomib. Immunoblots show expression of GFP^u protein, with PCNA as a loading control. GFP-u1 cells were either untreated (–) or treated with increasing concentrations (in nM) of bortezomib for 48 hr as indicated. Cells were also treated with the protease inhibitors aprotinin (A), leupeptin (L), or pepstatin (P) as a control.

(E) GFP-u1 cells express GFP^u after treatment with HDAC inhibitors. Immunoblots show expression of GFP^u, with PCNA as a loading control. GFP-u1 cells were untreated (–) or treated with aprotinin (A, 1 μg/ml), TSA, SAHA, or PXD101 for 48 hr as indicated. The fold change relative to mock for TSA, SAHA, and PXD101 was 33, 24, 20, 22, 23, and 34 (lanes 3–8, respectively).

(F) RT-PCR showing levels of GFP RNA after treatment of GFP-u1 cells for 48 hr with bortezomib, MG132, SAHA, or TSA as indicated; M indicates mock treatment. 18S rRNA levels were used as a loading control. The fold change in GFP RNA relative to 18S rRNA is shown underneath; – indicates the no-primer control.

(Ga) Purified proteasomes were incubated with vehicle (■), SAHA (□), PXD101 (●), or bortezomib (△) for 10 min prior to fluorogenic substrate addition. Cleaved substrate representative of active proteasome was measured at 2 min intervals for 60 min. Data are presented in arbitrary fluorescent units (AFU).

(Gb) U2OS cells were treated with vehicle (◆), SAHA (■), or bortezomib (▲) and harvested at 4 hr, when HR23B levels had begun to change. Purified proteasomes were then incubated with fluorogenic substrate. Cleaved substrate representative of active proteasome was measured at 2 min intervals for 18 min. n = 3; error bars = SD.

(H) GFP-u1 cells were treated under mock conditions or with SAHA (30 μM) and either nontargeting control (NT; 100 nM) or HR23B siRNA (as indicated in nM), and the levels of GFP, HR23B, and actin (as a loading control) were measured by immunoblotting at 48 hr.

HR23B hinders the degradation of GFP^u in HDAC inhibitor-treated cells. Since GFP^u is degraded via the proteasome (Bence et al., 2001) (Figure 3D), these results support the idea that reduced levels of HR23B reinstate proteasome activity in HDAC inhibitor-treated cells.

The proteasome is becoming increasingly recognized as a viable cancer target, and a variety of small-molecule drugs that interfere with proteasome activity are either in development or already approved for clinical use (Nalepa et al., 2006). In a fashion similar to HDAC inhibitors, proteasome inhibitors

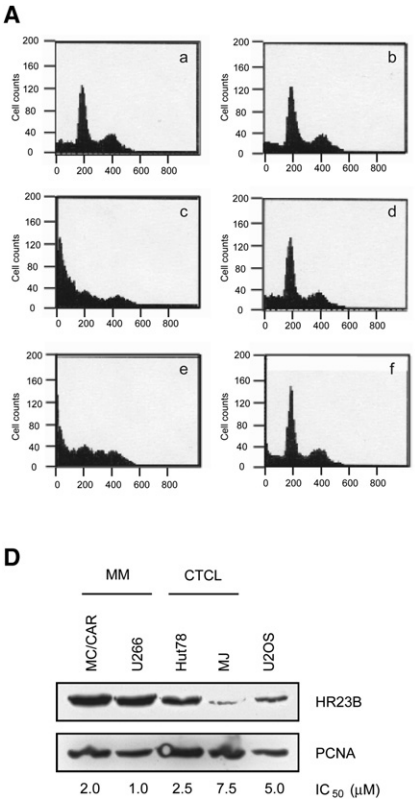

	siRNA	Phase subG1	G1	S	G2/M
untreated	lamin	11.69	57.94	4.57	26.07
	HR23B	9.36	62.15	4.4	24.35
SAHA	lamin	64.98	21.56	2.02	11.75
	HR23B	13.08	63.05	4.09	19.29
MG132	lamin	37.91	31.06	6.22	25.33
	HR23B	11.55	63.7	3.77	21.31

Figure 4. HDAC Inhibitors, Proteasome Inhibitors, and HR23B

(Aa–Af) HR23B depletion leads to rescue of HDAC inhibitor- and proteasome inhibitor-mediated apoptosis. FACS profiles depict the effect of treatment of U2OS cells with either lamin (Aa, Ac, and Ae) or HR23B (Ab, Ad, and Af) siRNA for 48 hr followed by a subsequent 48 hr treatment with normal culture medium or medium containing 5 μM SAHA (Ab and Ad) or 0.5 μM MG132 (Ae and Af). Cell viability is shown in Figure S2E.

(B) Quantitation of FACS profiles presented in (A).

(C) Immunoblot showing protein levels of HR23B, lamin, and PCNA for the experiment described in (A).

(D) Levels of HR23B in multiple myeloma (MM) and cutaneous T cell lymphoma (CTCL) cell lines and HDAC inhibitor sensitivity. Extracts from the indicated cell lines were immunoblotted with anti-HR23B as indicated, with PCNA as a loading control. The HDAC inhibitor IC_{50} of each cell line is indicated below, and the effect of the HDAC inhibitor on the cell-cycle profile is shown in Figure S2F.

cause profound apoptosis in tumor cells (Richardson et al., 2006). Since HR23B is likely to be responsible for the altered proteasome activity observed in HDAC inhibitor-treated cells, we surmised that HR23B might also influence the sensitivity of cells to proteasome inhibitors. Indeed, HR23B siRNA caused a dramatic reduction in the level of apoptosis induced by the proteasome inhibitor MG132 in U2OS cells (Figures 4A–4C). Furthermore, HR23B was induced upon treating U2OS cells with the proteasome inhibitor MG132 (Figure 2G; Figure 4C), reaching levels similar to those seen in cells treated with HDAC inhibitors. HR23B is therefore functionally important in mediating tumor cell sensitivity to both HDAC and proteasome inhibitor drugs, suggesting that HDAC and proteasome inhibitors act on overlapping pathways.

HR23B Expression in Clinical CTCL Biopsies

Although it remains unclear which tumors undergo a favorable clinical response to HDAC inhibitors, the hematological malignancy cutaneous T cell lymphoma (CTCL) has to date been found to be particularly sensitive to HDAC inhibitor-based therapies (Duvic and Zhang, 2006; Mann et al., 2007). We therefore evaluated HR23B levels in tumor cell lines derived from hematological malignancies and thereafter evaluated their sensitivity to HDAC inhibitors. In a small panel of cell lines derived from CTCL and multiple myeloma (MM), HR23B levels correlated with sensitivity to SAHA (Figure 4D; Figure S2F). Following on this, it was of interest to examine HR23B in clinical biopsies taken from patients suffering from CTCL. By immunohistochemistry in biopsy-verified CTCL, including mycosis fungoides and its leukemic variant Sézary syndrome, HR23B was expressed at high levels (Table 1). The expression of HR23B was localized to malignant CD3-positive T cells and areas of tumor mass (Figure 5). Since some CTCL biopsies expressed low levels of HR23B (Table 1), HR23B expression is not a general feature of CTCL. Moreover, HR23B levels were low in nonmalignant tissue in which activated T cells were present (according to anti-CD3 staining), such as chronic dermatitis (Table 1; Figure 6A), and thus HR23B expression is not a marker of activated T cells. HR23B is therefore highly expressed in malignant T cells in CTCL in situ, which represents a malignancy that is known to be sensitive to HDAC inhibitor-based therapies.

DISCUSSION

The Proteasome and HDAC Inhibitors

HDACs were originally regarded as a family of enzymes that act principally at the epigenetic level by regulating histone acetylation, and therefore HDAC inhibitors were believed to cause cell killing through influencing epigenetic control (Marks and Jiang, 2005; Inche and La Thangue, 2006). However, a variety of non-histone and non-chromatin-associated proteins have since been found to be acetylated, such that acetylation is presently regarded more as a pleiotropic level of posttranslational modification than one that is specifically associated with epigenesis (Chan and La Thangue, 2001; Bolden et al., 2006; Xu et al., 2007). Our study bears on the mechanisms through which HDAC inhibitors kill tumor cells. Numerous mechanisms have been proposed to explain HDAC inhibitor-induced cell death, such as upregulation of death receptors, effects on angiogenesis, and regulation of cell-cycle checkpoints (Minucci and Pelicci, 2006; Bolden et al., 2006; Xu et al., 2007). The results presented here raise the possibility that aberrant proteasome

Table 1. Summary of HR23B Expression in CTCL Together with Characteristics of Abnormal T Cells

Histology Number	CTCL Diagnosis	Neoplastic Cells Positive for HR23B	Neoplastic Cells Negative for HR23B	Characteristics
1	mycosis fungoides		+	CD3+, CD4+
2	mycosis fungoides	+		
3	Sézary syndrome	+		CD3+, CD8+
4	mycosis fungoides	+		
5	mycosis fungoides	+		concomitant lymphomatoid papulosis
6	mycosis fungoides	+		
7	mycosis fungoides	+		CD2+, CD3+, CD30+
8	mycosis fungoides	+		CD30+
9	mycosis fungoides	+		CD3+, CD30+
10	mycosis fungoides	+		CD2+, CD4+, CD5+, CD30+
11	cutaneous cytotoxic T cell lymphoma	+		CD8+
12	cutaneous anaplastic large cell lymphoma	+		CD30+
13	cutaneous lymphoproliferative disorder	+		CD30+
14	cutaneous lymphoproliferative disorder	+		CD4+, CD8+, CD30+
15	cutaneous lymphoproliferative disorder	+		CD30+
16	low-grade T cell lymphoma		+	
17	chronic dermatitis		(+)	

Diagnosis of disease is indicated. A biopsy taken from chronic dermatitis (histology number 17) showed a high infiltration of inflammatory nonmalignant T cells, indicated as (+), that expressed low levels of HR23B (see Figure 6A).

activity contributes to the killing process because HR23B, identified through a genome-wide loss-of-function screen for genes that govern sensitivity to HDAC inhibitor-induced apoptosis, is functionally important in mediating the effect of HDAC inhibitors. Specifically, depleting HR23B reduced the sensitivity of tumor cells to apoptosis resulting from HDAC inhibitors. While HR23B functions in shuttling cargo proteins to the proteasome as well as in NER (Sugasawa et al., 1997; Chen et al., 2001), our evidence suggests that it is the proteasome shuttling activity that is the important property in HDAC inhibitor-treated cells. It is consistent with this idea that the association between HR23B and the proteasome increased, and that proteasome activity was compromised, in HDAC inhibitor-treated cells. Importantly, the level of HR23B had a direct influence on protein turnover mediated by the proteasome because depleting HR23B reinstated proteasome activity in HDAC inhibitor-treated cells. Proteasome activity therefore appears to be regulated in HDAC inhibitor-treated cells through a process that involves HR23B (Figure 6B). While these results do not exclude other mechanisms and pathways contributing to HDAC inhibitor-induced cell death (Richon, 2006; Bolden et al., 2006), they do strongly implicate HR23B and the proteasome as components of a pathway that is under aberrant control in cells treated with HDAC inhibitors.

HDAC Inhibitors in the Clinical Setting

In addition to its effects in HDAC inhibitor-treated cells, HR23B governs the susceptibility of tumor cells to drugs that act directly on the proteasome. While this observation is of intrinsic interest, it also lends support to the idea that HDAC inhibitors influence proteasome activity, and furthermore that HDAC and proteasome inhibitors induce apoptosis through overlapping mechanisms. The latter point is particularly relevant and could have importance in the clinical setting, where combination therapies are frequently employed to achieve maximum clinical effect. In a therapy involving an HDAC inhibitor and proteasome inhibitor, a delicate balance of drug dose and scheduling might be required to achieve the necessary level of proteasome inhibition to mediate antitumor activity.

Although numerous ideas have been proposed (Duvic and Zhang, 2006; Richon, 2006; Xu et al., 2007), the mechanism or mechanisms through which HDAC inhibitors exert antitumor activity in CTCL are not known. Consequently, it remains unclear whether CTCL is the sole malignancy that is unusually sensitive to HDAC inhibitors or alternatively represents one of many malignancies yet to be proven sensitive. As phase 2 proof-of-concept clinical studies become available, it will become possible to evaluate this important question. However, clinical trials are often lengthy, and equally importantly, it is a challenging exercise to predict tumor response to the therapy under investigation without an informative biomarker. It might be possible to accelerate our knowledge of the clinical spectrum of responsive tumors if biomarkers that act in a predictive fashion can be identified. The expression of HR23B in tumors could offer such an opportunity, and by correlating expression level with clinical response, it should be possible to evaluate this idea.

In conclusion, we have used a genome-wide loss-of-function screening approach to interrogate the mechanisms of HDAC inhibitor-induced cell death. Our study has unearthed a pathway, involving proteasome activity and the proteasome-targeting activity of HR23B, that is altered in HDAC inhibitor-treated cells. The results point toward a level of control mediated via the proteasome that contributes to the anticancer activity of HDAC inhibitor-based therapies.

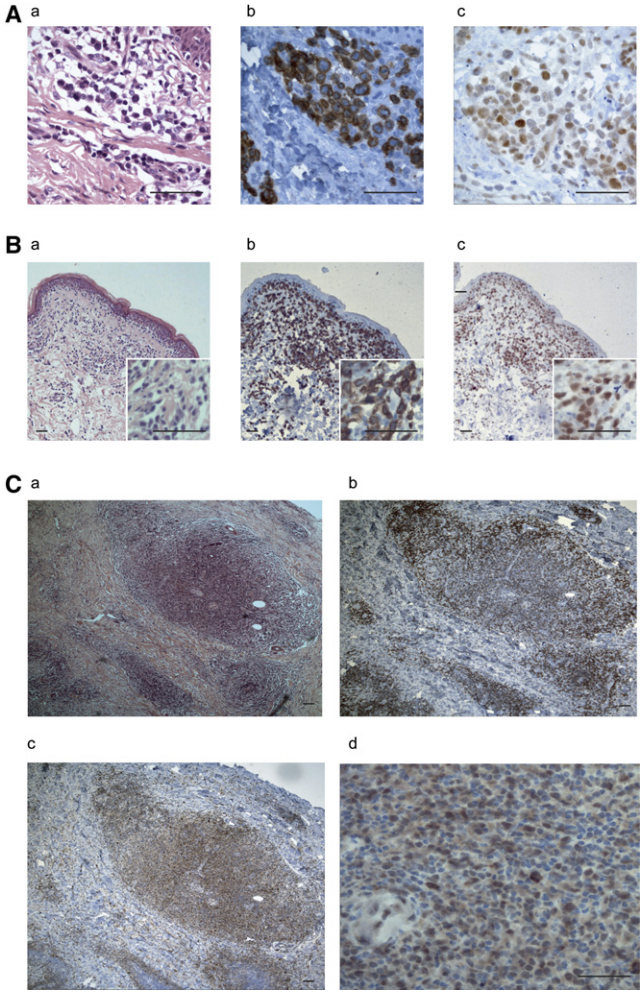

Figure 5. Expression of HR23B in Cutaneous T Cell Lymphoma In Situ

(A and B) Examples of tissue sections taken from CTCL biopsies showing hematoxylin and eosin staining (left), anti-CD3 immunostaining (middle), and anti-HR23B immunostaining (right).

(A) Mycosis fungoides (histology number 7).

(B) Cutaneous cytotoxic T cell lymphoma (histology number 11). Insets show increased magnifications taken from the corresponding images.

(Ca–Cd) Cutaneous lymphoproliferative disorder (histology number 13). Note that the intensely stained malignant (CD3-positive) T cells in (Cb) correspond with areas of HR23B staining in (Cc). (Cd) shows an increased magnification of the tumor mass in (Cb). In (Aa)–(Ac), (Ba)–(Bc), and (Ca)–(Cc), each image in the triplet represents a separate serial section from the biopsy.

Scale bars = 50 μm.

EXPERIMENTAL PROCEDURES

pRetroSuper shRNA Loss-of-Function Screen

Viral pools were produced by transfection of Phoenix packaging cells with the pRetroSuper shRNA library (Berns et al., 2004) using calcium phosphate precipitation. U2OS cells expressing the murine ecotropic receptor (U2OSEcR) were then infected with the viral pools. Cells were grown for 72 hr to allow for shRNA expression and then plated overnight (40,000 cells per plate). Suberoylanilide hydroxamic acid (SAHA; 2 μM) was then added to each plate. SAHA-containing medium was replaced every 3 days for 25 days until the appearance of colonies on plates treated with SAHA and viral library. Colonies were then picked and expanded to allow isolation of total genomic DNA and protein. Genomic DNA was isolated from surviving cells as described previously (Berns et al., 2004).

The complete shRNA library (Berns et al., 2004) was screened. From the primary screen, 132 colonies were isolated, and of these, about 17 grew in 2 μM SAHA (Figure S1). The shRNA inserts were identified by PCR. Several colonies contained multiple shRNA vectors and were deprioritized. Six colonies failed to grow, or grew very slowly. *HR23B* (gene ID NM_002874) and the remaining 11 genes identified (gene IDs NM_002411, NM_002123, NM_002855, NM_016186, NM_000521, NM_002300, NM_002309, NM_002310, NM_002372, NM_016445, and NM_013352) are summarized in Figure S1.

Pathology Examination

CTCL diagnosis was verified by examination by three independent pathologists. Paraffin-embedded formalin-fixed tissues from 15 CTCLs were sectioned (5 μm) onto glass slides, cleared of paraffin in Citroclear, and rehydrated through graded alcohol baths. After a rinse in water, sections were "pressure cooked" for 2 min in 1 mM EDTA at pH 8 for heat-induced epitope retrieval. Slides were incubated in 0.03% hydrogen peroxide for 5 min to inactivate endogenous peroxidases, incubated with 0.1% Triton for 10 min to improve antibody penetration, and treated with anti-HR23B or anti-CD3 followed by rabbit anti-mouse HRP secondary antibody and then substrate (DAB; DAKO). Slides were placed in hematoxylin (Sigma) for 1–2 s for nuclear counterstaining and then mounted with coverslips using AquaTex (Merck). Sections were examined under a Zeiss Axioskop light microscope. Images were captured with MicroPublisher 5.0 RTV, and imaging was performed with Adobe Photoshop 8.0. Use of human tissues in this study was approved by the Oxfordshire Research Ethics Committee (ref. no. CO2.216).

Proteasome Assay

The proteasome assay components were reconstituted and stored under conditions described by BIOMOL International. Assay buffer was added to each well as follows: 40 μl in blank (no proteasome), 30 μl in control (no inhibitor), and 25 μl in inhibitor wells. 20S purified proteasome (10 μl) from human erythrocytes was added to all wells except blanks. SAHA (5 μM), PXD101 (1 μM), bortezomib (90 nM), and epoxomicin (0.5 μM) were added to all wells except blanks and controls. Following 10 min incubation at room temperature, 10 μl Suc-LLVY-AMC substrate, which measures chymotrypsin-like peptidase activity, was added to all wells. The plate was read every 2 min for 1 hr using a plate reader (360 nm excitation, 460 nm emission, gain = 58).

Assay for Proteasome Activity from HDAC Inhibitor-Treated Cells

U2OS cells were harvested after 4 hr of treatment with SAHA (5 μM), PXD101 (1 μM), bortezomib (90 nM), or vehicle control. Following a wash in 1× PBS, cells were resuspended in 100 μl HEPES buffer (5 mM HEPES, 1 mM EDTA [pH7.5]) and sonicated for 1 min. Samples were centrifuged for 10 min (14,000 rpm at 4°C) and the supernatant was removed, stored on ice, and used immediately. Proteasome activity per sample was measured by adding 30 μl cell lysate to each well in triplicate. Assay buffer (40 μl) was added as a blank. The fluorogenic substrate Suc-LLVY-AMC was added to all samples and incubated for 10 min at room temperature. The plate was read every 2 min for 1 hr on a plate reader (360 nm excitation, 460 nm emission, gain = 58).

SUPPLEMENTAL DATA

The Supplemental Data include Supplemental Experimental Procedures and three figures and can be found with this article online at http://www.cancercell.org/supplemental/S1535-6108(08)00406-6.

ACKNOWLEDGMENTS

We thank the Medical Research Council (MRC) and Cancer Research UK (CRUK) for supporting this work, R. Williams for assistance in preparing the manuscript, and H. Turley for technical assistance. Research in our laboratory is supported by the MRC, CRUK, the Association for International Cancer Research, the Leukaemia Research Fund, and the European Union.

N.B.L.T. is a founder of Celleron Therapeutics.

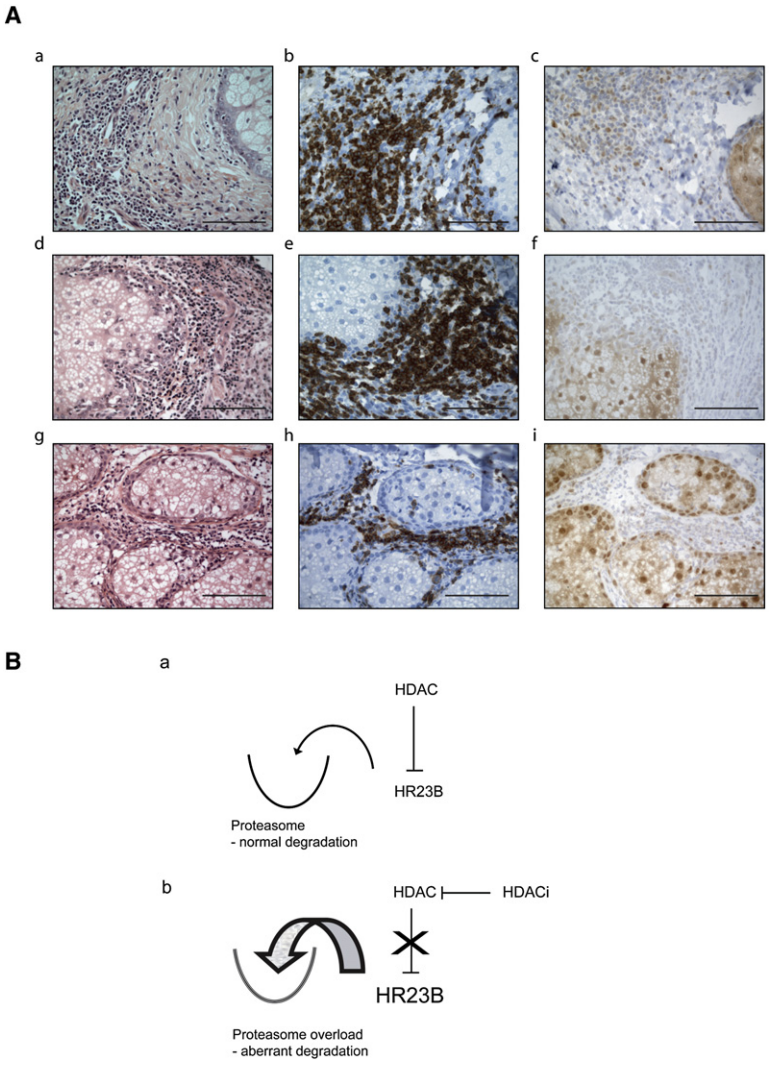

Figure 6. Expression of HR23B in Tissue In Situ

(Aa–Ai) Tissue sections from biopsies taken from mycosis fungoides (Aa–Ac; histology number 1), chronic dermatitis (Ad–Af; histology number 17), and a nonmalignant perivascular T cell (CD3-positive) infiltrate surrounding an apocrine gland (Ag–Ai) showing hematoxylin and eosin staining (left panels), anti-CD3 staining (middle panels), and anti-HR23B staining (right panels). Note that the malignant (CD3-positive) T cells in the mycosis fungoides (Ab) have low levels of HR23B (Ac). Similarly, the T cell (CD3-positive) infiltrates in (Ae) and (Ah) exhibit low levels of HR23B immunostaining. Scale bars = 50 μm.

(Ba and Bb) HDAC is functionally important in regulating HR23B. It is proposed that HDAC influences HR23B activity, which is required for normal proteasome function (Ba). Upon HDAC inhibition (HDACi), increased HR23B activity provokes abnormal protein turnover by causing aberrant proteasome activity, perhaps by saturating the proteasome (Bb).

Received: April 2, 2008
Revised: October 8, 2008
Accepted: December 2, 2008
Published: January 5, 2009

REFERENCES

Bence, N.F., Sampat, R.M., and Kopito, R.R. (2001). Impairment of the ubiquitin-proteasome system by protein aggregation. Science *292*, 1552–1555.

Berns, K., Hijmans, E.M., Mullenders, J., Brummelkamp, T.R., Velds, A., Heimerikx, M., Kerkhoven, R.M., Madiredjo, M., Nijkamp, W., Weigelt, B., et al. (2004). A large-scale RNAi screen in human cells identifies new components of the p53 pathway. Nature *428*, 431–437.

Bolden, J.E., Peart, M.J., and Johnstone, R.W. (2006). Anticancer activities of histone deacetylase inhibitors. Nat. Rev. Drug Discov. *5*, 769–784.

Carey, N., and La Thangue, N.B. (2006). Histone deacetylase inhibitors: gathering pace. Curr. Opin. Pharmacol. *6*, 369–375.

Chan, H.M., and La Thangue, N.B. (2001). p300/CBP proteins: HATs for transcriptional bridges and scaffolds. J. Cell Sci. *114*, 2363–2373.

Chen, L., and Madura, K. (2002). Rad23 promotes the targeting of proteolytic substrates to the proteasome. Mol. Cell. Biol. *22*, 4902–4913.

Chen, L., Shinde, U., Ortolan, T.G., and Madura, K. (2001). Ubiquitin-associated (UBA) domains in Rad23 bind ubiquitin and promote inhibition of multiubiquitin chain assembly. EMBO Rep. *2*, 933–938.

Duvic, M., and Zhang, C. (2006). Clinical and laboratory experience of vorinostat (suberoylanilide hydroxamic acid) in the treatment of cutaneous T-cell lymphoma. Br. J. Cancer *95* (*Suppl 1*), S13–S19.

Fujiwara, K., Tenno, T., Sugasawa, K., Jee, J.G., Ohki, I., Kojima, C., Tochio, H., Hiroaki, H., Hanaoka, F., and Shirakawa, M. (2004). Structure of the ubiquitin-interacting motif of S5a bound to the ubiquitin-like domain of HR23B. J. Biol. Chem. *279*, 4760–4767.

Gilon, T., Chomsky, O., and Kulka, R.G. (1998). Degradation signals for ubiquitin system proteolysis in Saccharomyces cerevisiae. EMBO J. *17*, 2759–2766.

Hiyama, H., Yokoi, M., Masutani, C., Sugasawa, K., Maekawa, T., Tanaka, K., Hoeijmakers, J.H., and Hanaoka, F. (1999). Interaction of hHR23 with S5a. The ubiquitin-like domain of hHR23 mediates interaction with S5a subunit of 26 S proteasome. J. Biol. Chem. *274*, 28019–28025.

Inche, A.G., and La Thangue, N.B. (2006). Chromatin control and cancer-drug discovery: realizing the promise. Drug Discov. Today *11*, 97–109.

Khan, O., and La Thangue, N.B. (2008). Drug Insight: histone deacetylase inhibitor-based therapies for cutaneous T-cell lymphomas. Nat. Clin. Pract. Oncol. *5*, 714–726.

Li, L., Bales, E.S., Peterson, C.A., and Legerski, R.J. (1993). Characterization of molecular defects in xeroderma pigmentosum group C. Nat. Genet. *5*, 413–417.

Mann, B.S., Johnson, J.R., Cohen, M.H., Justice, R., and Pazdur, R. (2007). FDA approval summary: vorinostat for treatment of advanced primary cutaneous T-cell lymphoma. Oncologist *12*, 1247–1252.

Marks, P.A., and Jiang, X. (2005). Histone deacetylase inhibitors in programmed cell death and cancer therapy. Cell Cycle *4*, 549–551.

Marks, P.A., and Breslow, R. (2007). Dimethyl sulfoxide to vorinostat: development of this histone deacetylase inhibitor as an anticancer drug. Nat. Biotechnol. *25*, 84–90.

Minucci, S., and Pelicci, P.G. (2006). Histone deacetylase inhibitors and the promise of epigenetic (and more) treatments for cancer. Nat. Rev. Cancer *6*, 38–51.

Nalepa, G., Rolfe, M., and Harper, J.W. (2006). Drug discovery in the ubiquitin-proteasome system. Nat. Rev. Drug Discov. *5*, 596–613.

Ng, J.M., Vrieling, H., Sugasawa, K., Ooms, M.P., Grootegoed, J.A., Vreeburg, J.T., Visser, P., Beems, R.B., Gorgels, T.G., Hanaoka, F., et al. (2002). Developmental defects and male sterility in mice lacking the ubiquitin-like DNA repair gene mHR23B. Mol. Cell. Biol. *22*, 1233–1245.

Richardson, P.G., Mitsiades, C., Hideshima, T., and Anderson, K.C. (2006). Bortezomib: proteasome inhibition as an effective anticancer therapy. Annu. Rev. Med. *57*, 33–47.

Richon, V.M. (2006). Cancer biology: mechanism of antitumour action of vorinostat (suberolyanilide hydroxamic acid), a novel deacetylase inhibitor. Br. J. Cancer *95* (*Suppl 1*), S2–S6.

Schauber, C., Chen, L., Tongaonkar, P., Vega, I., Lambertson, D., Potts, W., and Madura, K. (1998). Rad23 links DNA repair to the ubiquitin/proteasome pathway. Nature *391*, 715–718.

Sugasawa, K., Ng, J.M., Masutani, C., Maekawa, T., Uchida, A., van der Spek, P.J., Eker, A.P., Rademakers, S., Visser, C., Aboussekhra, A., et al. (1997). Two human homologs of Rad23 are functionally interchangeable in complex formation and stimulation of XPC repair activity. Mol. Cell. Biol. *17*, 6924–6931.

Wilkinson, C.R., Seeger, M., Hartmann-Petersen, R., Stone, M., Wallace, M., Semple, C., and Gordon, C. (2001). Proteins containing the UBA domain are able to bind to multi-ubiquitin chains. Nat. Cell Biol. *3*, 939–943.

Xu, W.S., Parmigiani, R.B., and Marks, P.A. (2007). Histone deacetylase inhibitors: molecular mechanisms of action. Oncogene *26*, 5541–5552.